FtsZ filaments have the opposite kinetic polarity of microtubules

Shishen Du[a], Sebastien Pichoff[a], Karsten Kruse[b,c,d], and Joe Lutkenhaus[a,1]

[a]Department of Microbiology, Molecular Genetics, and Immunology, University of Kansas Medical Center, Kansas City, KS 66160; [b]Department of Biochemistry, University of Geneva, 1211 Geneva, Switzerland; [c]Department of Theoretical Physics, University of Geneva, 1211 Geneva, Switzerland; and [d]The National Center of Competence in Research Chemical Biology, University of Geneva, 1211 Geneva, Switzerland

Contributed by Joe Lutkenhaus, August 29, 2018 (sent for review July 11, 2018; reviewed by Jan Löwe and Jie Xiao)

FtsZ is the ancestral homolog of tubulin and assembles into the Z ring that organizes the division machinery to drive cell division in most bacteria. In contrast to tubulin that assembles into 13 stranded microtubules that undergo dynamic instability, FtsZ assembles into single-stranded filaments that treadmill to distribute the peptidoglycan synthetic machinery at the septum. Here, using longitudinal interface mutants of FtsZ, we demonstrate that the kinetic polarity of FtsZ filaments is opposite to that of microtubules. A conformational switch accompanying the assembly of FtsZ generates the kinetic polarity of FtsZ filaments, which explains the toxicity of interface mutants that function as a capper and reveals the mechanism of cooperative assembly. This approach can also be employed to determine the kinetic polarity of other filament-forming proteins.

FtsZ | capper | Z ring | treadmilling | tubulin

Prokaryotic cytoskeletons play essential roles in many fundamental aspects of prokaryotic cell biology, including cytokinesis, cell-shape maintenance, chromosome segregation, and other aspects of cellular organization (1). FtsZ, a prokaryotic tubulin homolog, polymerizes into filaments that coalesce into the Z ring at midcell (2–4). The ring functions as a scaffold for recruitment of the machinery necessary to synthesize septal peptidoglycan (5, 6). Since formation of the Z ring is the first step in bacterial cytokinesis, antagonism of FtsZ polymerization is a prominent mechanism for regulating cell division in bacteria (7–11).

Like tubulin, FtsZ undergoes GTP-dependent, cooperative assembly with a critical concentration of about 1 μM (12, 13). However, FtsZ differs from tubulin in several ways. Tubulin is present as an αβ-heterodimer that assembles into microtubules containing 13 protofilaments (14), whereas FtsZ is a monomer that polymerizes into single-stranded filaments in vitro of about 120–200 nm in length (30–50 subunits) under conditions that best mimic in vivo conditions (5, 15). In vivo, FtsZ assembles into small clusters of filaments of unknown structure that together compose the Z ring (16, 17). Furthermore, microtubules undergo dynamic instability (18), whereas FtsZ filaments treadmill (16, 19). FtsZ filaments form the scaffold for the divisome, and the treadmilling distributes this peptidoglycan synthetic machinery around the septum (16, 20). FtsZ exists in two conformations: an open conformation observed in filaments and a closed conformation in the monomer (21). The basis of treadmilling is an assembly-associated conformational switch that promotes polymerization along with the assembly-associated GTP hydrolysis that weakens intersubunit interactions (21). However, the kinetic polarity of these FtsZ filaments, or how it is achieved, is not known (5).

Dynamic filaments have structural and kinetic polarity. The growing end is referred to as the "plus" end and the other end is referred to as the "minus" end. When tubulin assembles into microtubules, the bound GTP (top end) is exposed at the plus end, and incoming subunits interact with this end through their T7 loop (bottom end) (14). Like tubulin, FtsZ assembles in a head-to-tail manner, however, there are several indications that the polarity of FtsZ assembly is opposite to that of microtubules.

Since FtsZ filaments treadmill, longitudinal interface mutants of FtsZ should have different effects on assembly. Interface mutants that can add to the growing end but prevent further growth should be toxic to assembly and thus cell division at substoichiometric levels, whereas interface mutants that cannot add onto filaments should be much less toxic. Redick et al. (22) observed that some amino acid substitutions at the bottom end of FtsZ were toxic, whereas substitutions at the top end were not. Furthermore, expression of just the N-terminal domain (1–193, top end), but not the C-terminal domain of FtsZ, showed some toxicity (23). Also, the N-terminal domain of FtsZ has been shown to antagonize FtsZ polymerization in vitro (24). These observations suggest that FtsZ filaments have the opposite kinetic polarity of microtubules; however, previous measurements showed that neither the bottom-face mutants nor the N-terminal domain of FtsZ was toxic at substoichiometric levels but needed to be overexpressed three-to fivefold (22, 23), arguing against this suggestion. Since the mutations examined in the prior study were made before the structure of an FtsZ filament was known, and many of the mutants still assembled in vivo, we decided to reinvestigate the effect of interface mutants using known mutations. Our findings demonstrate that the kinetic polarity of FtsZ filaments is the opposite of tubulin assembly into microtubules. Furthermore, we propose how the conformational switch coupled to assembly promotes polymerization.

Significance

FtsZ is the founding member of the prokaryotic tubulin family. It assembles into single-stranded filaments that coalesce to form the Z ring that drives bacterial cell division in most bacteria. FtsZ filaments undergo cooperative assembly and display treadmilling behavior. Here we investigate the kinetic polarity of FtsZ filaments by studying the toxicity of longitudinal interface mutants of FtsZ and find that bottom-face mutants are extremely toxic. This toxicity combined with a conformational switch induced during assembly reveals the kinetic polarity of FtsZ filaments, the basis for cooperative assembly, and explains the basis for other inhibitors of FtsZ assembly. It is likely that all members of the FtsZ/tubulin superfamily employ an assembly-induced conformational switch to generate kinetic polarity, which could be revealed by the same approach used here.

Author contributions: S.D. and J.L. designed research; S.D., S.P., and K.K. performed research; S.P. contributed new reagents/analytic tools; S.D., K.K., and J.L. analyzed data; and S.D. and J.L. wrote the paper.

Reviewers: J.L., Medical Research Council Laboratory of Molecular Biology; and J.X., Johns Hopkins University School of Medicine.

The authors declare no conflict of interest.

Published under the PNAS license.

[1]To whom correspondence should be addressed. Email: jlutkenh@kumc.edu.

This article contains supporting information online at www.pnas.org/lookup/suppl/doi:10.1073/pnas.1811919115/-/DCSupplemental.

Published online October 1, 2018.

Results

Strategy for Determining Polarity of FtsZ Filaments. The expected effect of top and bottom interface mutants on treadmilling of FtsZ is outlined in Fig. 1*A*. In the first scenario, FtsZ polymerizes in the same direction as tubulin (top-end growth), and a top interface mutant would add to the growing or plus end blocking the growth of the filament, resulting in disassembly. Such a mutant would be expected to be dominant-negative and inhibit cell division, whereas a bottom interface mutant would not affect polymerization and thus would be nontoxic. In the second scenario, FtsZ polymerizes in the opposite direction of tubulin (bottom-end growth), and the effects of the top- and bottom-face mutants on polymerization and cell division would be reversed. Li et al. (25) described interface mutants that are unable to assemble including top [FtsZ$^{L178E(top)}$] and bottom-face mutants [FtsZ$^{L272E(bottom)}$]. These mutants do not assemble because charged residues would be forced into hydrophobic pockets formed between subunits in the filament (Fig. 1*B*).

The Bottom Interface Mutant Is Toxic at Substoichiometric Levels. Two plasmid vectors were used to express the *ftsZ* alleles: one expressed the alleles under the control of an arabinose-inducible promoter and the other under the control of an isopropyl β-D-thiogalactopyranoside (IPTG)-inducible promoter. Initially, the two interface mutations, *ftsZ*^{L178E} and *ftsZ*^{L272E}, were introduced into pSEB135 (P$_{ara}$::*ftsZ*) and tested for their ability to complement a depletion strain [SD18 *ftsZ*^{o} *recA56/repA*^{Ts} (P$_{ftsZ}$::*ftsZ*)] that has *ftsZ* provided by a temperature-sensitive plasmid. We also included *ftsZ*^{360}, an allele deleted for the conserved tail of *ftsZ* that mediates interaction with multiple FtsZ partners (26), the expression of which is known to be toxic (27). We confirmed that these three alleles were unable to complement the depletion strain at the nonpermissive temperature of 42 °C (*SI Appendix*, Fig. S1). Furthermore, we observed that expression of *ftsZ*^{L272E} and *ftsZ*^{360} was toxic at 30 °C, whereas expression of *ftsZ*^{178E} was not. By tagging the proteins with GFP, we confirmed that FtsZ^{L178E} and FtsZ^{L272E} were unable to polymerize in vivo (unable to localize to midcell) (*SI Appendix*, Fig. S2*A*). Furthermore, we confirmed that the purified proteins were unable to polymerize in vitro (*SI Appendix*, Fig. S2*B*).

Although arabinose-inducible vectors offer some advantages (tighter off regulation), they have some disadvantages (variable cell-to-cell induction) (28). To better assess the toxicity of *ftsZ*^{L272E}, we attempted to clone it into an IPTG-inducible vector; however, we were unsuccessful. Since this was likely due to toxicity from leaky expression, we modified the ribosome binding site for *ftsZ* on the plasmid to reduce expression (from CGGAGA to CGCAGA). Following this change, we were able to clone all *ftsZ* alleles into the IPTG-inducible vector. Induction of *ftsZ*^{L272E} and *ftsZ*^{360} from this plasmid was toxic with *ftsZ*^{L272E} being much more toxic (Fig. 2*A*). Induction of *ftsZ*^{L272E} in a WT strain caused filamentation and blocked colony formation at 30 μM IPTG (Fig. 2 *A* and *B*). Since induction of *ftsZ* with 1 mM IPTG from this plasmid does not provide enough FtsZ to fully complement a *ftsZ*-depletion strain (*SI Appendix*, Fig. S3), we conclude that FtsZ^{L272E} is inhibitory at substoichiometric levels. If the toxicity of FtsZ^{L272E} is due to incorporation into filaments, then addition of the L178E substitution to disrupt the other longitudinal interface should prevent incorporation into the polymer and alleviate the toxicity. Indeed, expression of the double mutant (*ftsZ*$^{LL/EE}$) did not block division and was not toxic (Fig. 2 *A* and *B*). The toxicity of FtsZ^{360}, which lacks the conserved C-terminal peptide that mediates interaction with multiple FtsZ partners (27), was also eliminated by addition of the L178E substitution, whereas addition of the L272E substitution increased the toxicity of FtsZ^{360} (Fig. 2 *A* and *B*). These results are consistent with L178E substitution preventing subunit addition to a filament whereas the L272E substitution likely allows subunit addition but prevents further growth of the filament.

As shown in Fig. 2*B* and *SI Appendix*, Fig. S4, induction of *ftsZ*^{L272E} with as little as 5 μM ITPG caused cells to elongate, and they became extremely filamentous with 20 μM IPTG even though the level of FtsZ did not increase significantly (endogenous FtsZ + induced FtsZ^{L272E}) (Fig. 2*C*). To determine the level of FtsZ^{L272E} necessary to cause toxicity, we measured the level of FtsZ$^{360(L272E)}$, which can be distinguished from full-length FtsZ, and found that, with 20 μM IPTG, its level was only 10% of the level of the endogenous FtsZ (Fig. 2*C*). This result confirms that FtsZ^{L272E} is toxic at a substoichiometric level. This result is in contrast to previous observations that bottom-face mutants had to be overexpressed

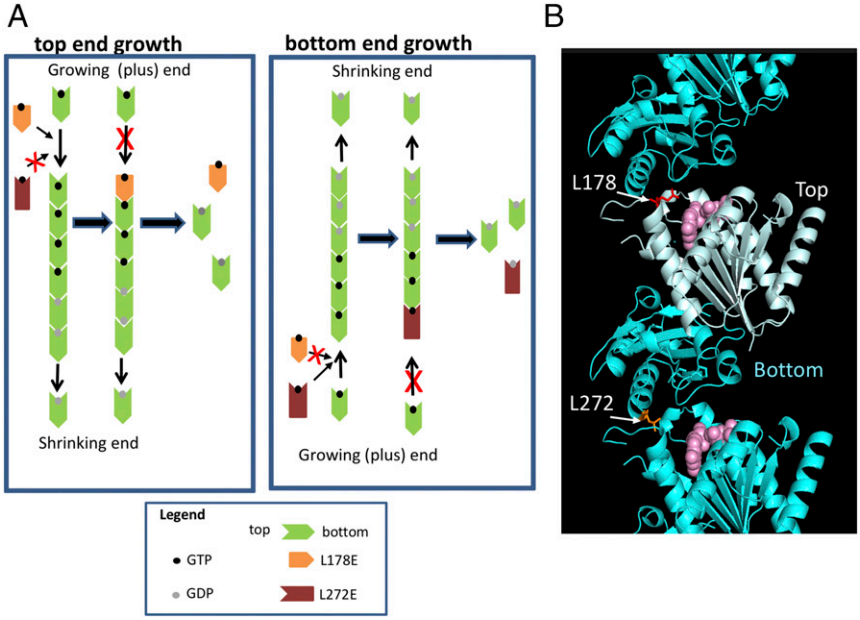

Fig. 1. FtsZ longitudinal interface mutants and the scheme used to determine FtsZ polymer polarity. (*A*) Two possible scenarios for the growth of FtsZ polymers. In the first case (top-end growth), FtsZ polymerizes in the same direction as tubulin with the bottom surface of an incoming subunit interacting with the top surface (GTP end) of the subunit at the growing end of a polymer, called the plus (+) end in tubulin. Subunits at the shrinking end dissociate from the filament following GTP hydrolysis. In this case, the top-surface mutant (FtsZ^{L178E}) adds to a treadmilling filament blocking further subunit addition resulting in disassembly from the shrinking end, while the bottom-surface mutant (FtsZ^{L272E}) does not have an effect. In the second situation, FtsZ polymerizes in the opposite direction of tubulin. In this case, the bottom-surface mutant FtsZ^{L272E} adds to the growing end of the filament and would block further growth, while the top-surface mutant does not have an effect. (*B*) FtsZ interface mutants used in this study. The FtsZ^{L178E} monomer was superimposed on the FtsZ filament from *Staphylococcus aureus* (PDB::3VOB). The GTP-binding domain (N-terminal) is the top interface (light cyan), while the domain containing the T7 synergy loop (C-terminal) is the bottom interface (dark cyan). GDP is pink.

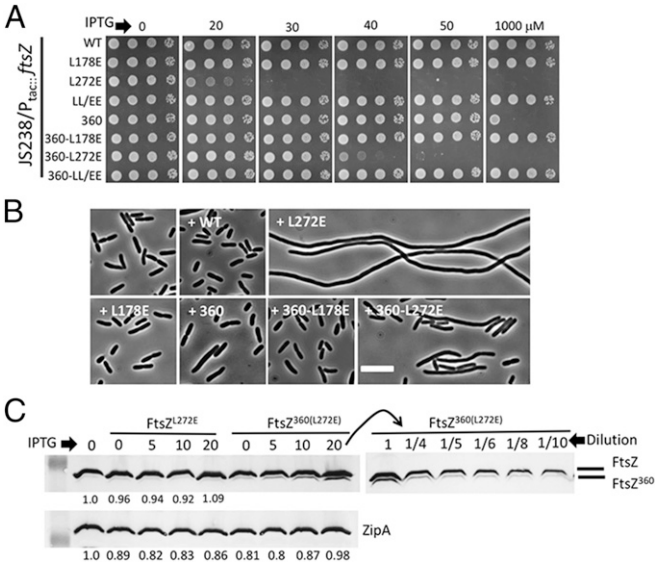

Fig. 2. The bottom-surface mutant (FtsZ^{L272E}) is dominant negative with substoichiometric toxicity. Plasmid pSD334 (P_{tac}::*ftsZ*) or derivatives containing different *ftsZ* alleles were transformed into strain JS238, and transformants were tested for toxicity. A 3-μL aliquot from each 10-fold serial dilution was spotted onto LB plates with chloramphenicol and IPTG and incubated at 37 °C overnight before imaging. (*B*) Cultures of some of the strains from *A* were induced with 30 μM IPTG for 2 h, and cells were photographed. (Scale bar: 5 μm.) (*C*) JS238-containing derivatives of pSD334 expressing *ftsZ*^{L272E} or *ftsZ*$^{360(L272E)}$ were induced with the indicated concentration of IPTG for 2 h, and a Western blot was performed to assess the level of the induced proteins. ZipA was blotted as a control. The sample from the 20-μM induction of *ftsZ*$^{360(L272E)}$ was serially diluted as indicated to assess the induced amount of FtsZ$^{360(L272E)}$ relative to the endogenous level of FtsZ. The level of FtsZ in the 1/10 dilution was about the level of FtsZ$^{360(L272E)}$ in the undiluted sample.

three- to fivefold to block colony formation using a plasmid with *ftsZ* under the control of an arabinose-inducible promoter (22). As shown in *SI Appendix*, Fig. S1, complementation with the arabinose-inducible promoter required 0.05–0.1% arabinose, but expression of *ftsZ*^{L272E} was already toxic to WT cells at 0.006% (*SI Appendix*, Fig. S5), consistent with FtsZ^{L272E} being toxic at substoichiometric levels.

FtsZ^{L272E} Incorporates into Z Rings to Cause Disruption. To understand how the FtsZ mutants blocked cell division, we expressed the various alleles of *ftsZ* under the control of the arabinose promoter and examined Z-ring formation using ZipA-GFP as a proxy. Following induction of WT FtsZ with 0.05% arabinose for 2 h, 91% of the cells had ZipA-GFP rings, whereas induction of FtsZ^{L272E} reduced the number of cells with ZipA-GFP rings to 0.7% (Fig. 3*A* and *SI Appendix*, Fig. S6*A*). Induction of FtsZ^{L178E} or FtsZ$^{LL/EE}$ had little effect (86 and 88% of cells with rings, respectively) even though they were induced to the same level (*SI Appendix*, Fig. S6 *B* and *C*). With induction of FtsZ^{360}, the percentage of cells with rings was reduced to 32% as many rings had started to spiral away, likely due to heteropolymers containing FtsZ^{360} (unable to bind to FtsZ's membrane tethers) poorly anchored to the membrane. Kinetic analysis revealed that Z rings started to disappear at 80 min after induction of FtsZ^{L272E} (*SI Appendix*, Fig. S7 *A* and *B*) before the level of FtsZ (FtsZ^{360} as a proxy) could be observed to increase (*SI Appendix*, Fig. S7*C*). These induction kinetics (rapid increase in the induced protein between 90 and 100 min) with the arabinose system are likely responsible for the previous underestimate of the toxicity (22).

To see if FtsZ^{L272E} localizes to Z rings before they are disrupted, we used *ftsZ*-mNeonGreen fusions [which are brighter than GFP (29)] expressed from the IPTG-inducible vector. Whereas FtsZ-mNeonGreen was readily observed in rings at midcell, FtsZ^{L272E}-mNeonGreen was not as easy to detect; however, we observed localization in some constricting cells. In contrast, no localization of FtsZ^{L178E}-mNeonGreen to the midcell was detected (Fig. 3*B*). Thus, FtsZ^{L272E} is incorporated into FtsZ polymers at the Z ring before the ring is disrupted.

FtsZ^{L272E} Blocks Polymerization of FtsZ. We next examined the effect of FtsZ^{L178E} and FtsZ^{L272E} on FtsZ polymerization in vitro using a sedimentation assay and electron microscopy. For the sedimentation test, we used FtsZΔCL, a variant of FtsZ (deletion of the long carboxy linker) that polymerizes well and can be distinguished from FtsZ^{L178E} and FtsZ^{L272E} on SDS/PAGE gels (30). FtsZΔCL sedimented in the presence of GTP, while FtsZ^{L178E}, FtsZ^{L272E}, and FtsZ$^{LL/EE}$ did not (*SI Appendix*, Fig. S8). Addition of FtsZ^{L178E} to FtsZΔCL did not affect the sedimentation of FtsZΔCL, whereas FtsZ^{L272E} reduced the amount of FtsZΔCL in the pellet in a dose-dependent manner (Fig. 4*A*). Adding the L178E substitution to FtsZ^{L272E} (FtsZ$^{LL/EE}$) eliminated its ability to antagonize FtsZΔCL sedimentation. Electron microscopy revealed that FtsZ^{L272E} (1:1 ratio) dramatically reduced the number of FtsZ or FtsZΔCL filaments (Fig. 4*B* and *SI Appendix*, Fig. S9, respectively) whereas FtsZ^{L178E} or FtsZ$^{LL/EE}$ did not have an effect. Since the addition of FtsZ^{L272E} to FtsZ (1:1 ratio) increased the GTPase activity (Fig. 4*C*) while dramatically reducing the number of filaments (Fig. 4*B*), sequestration is ruled out and suggests that short filaments (of a few subunits) not detected in the EM are capable of GTPase activity. Importantly, the addition of L178E to FtsZ^{L272E} (FtsZ$^{LL/EE}$) reduced the ability of FtsZ^{L272E} to stimulate the GTPase activity. FtsZ^{L178E} also increased the GTPase activity but to a lesser extent than FtsZ^{L272E} did. FtsZ^{L178E} likely stimulates the GTPase because it can participate in nucleation (being the first subunit in a filament). However, it is possible that FtsZ^{L178E} and FtsZ$^{LL/EE}$ retain weak interaction with FtsZ that is sufficient to stimulate the GTPase activity. Together, these results are consistent with the bottom-face mutant capping the end of the filament to block subunit addition leading to disassembly of the filament.

Computation Model for FtsZ Treadmilling. To further assess the impact of FtsZ^{L272E} on FtsZ assembly, we employed a computational model for treadmilling (31, 32) based upon what is known about FtsZ assembly (*Materials and Methods*). This model accounts for the following processes: (*i*) GTP subunit attachment at the bottom end and GDP subunit detachment at the top end, (*ii*) conversion of GTP to GDP subunits within the filament, and (*iii*) the attachment of mutant subunits that cap the filament and prevent further binding of subunits to the bottom end. Also, hydrolysis occurs at a constant rate, and there is no impact on the hydrolysis rate by the state of neighboring subunits in the filament. The parameters are k_A (rate for GTP subunit attachment), k_D (rate for GDP subunit detachment), k_H for the GTPase, and f (ratio of FtsZ mutant to FtsZ). With the parameters used, the average length of FtsZ filaments is 55 subunits with a range from 25 to over 100 (Fig. 5*A*). As FtsZ^{L272E} is titrated in, the average length starts to decrease in a dose-dependent manner. At a ratio of 1:10 (FtsZ^{L272E} to WT), the average length of FtsZ polymers is reduced about 75%. This result would be consistent with FtsZ^{L272E} reducing polymer length in vivo leading to dissolution of the Z ring. If so, increasing the amount of FtsZ should provide some resistance to FtsZ^{L272E} due to an increase in the ratio of FtsZ to FtsZ^{L272E}. Indeed, adding a plasmid that increases the level of FtsZ about twofold (33) increased the concentration of IPTG (and therefore the amount of FtsZ^{L272E}) required to prevent colony formation from 30 to 60 μM (Fig. 5*B*).

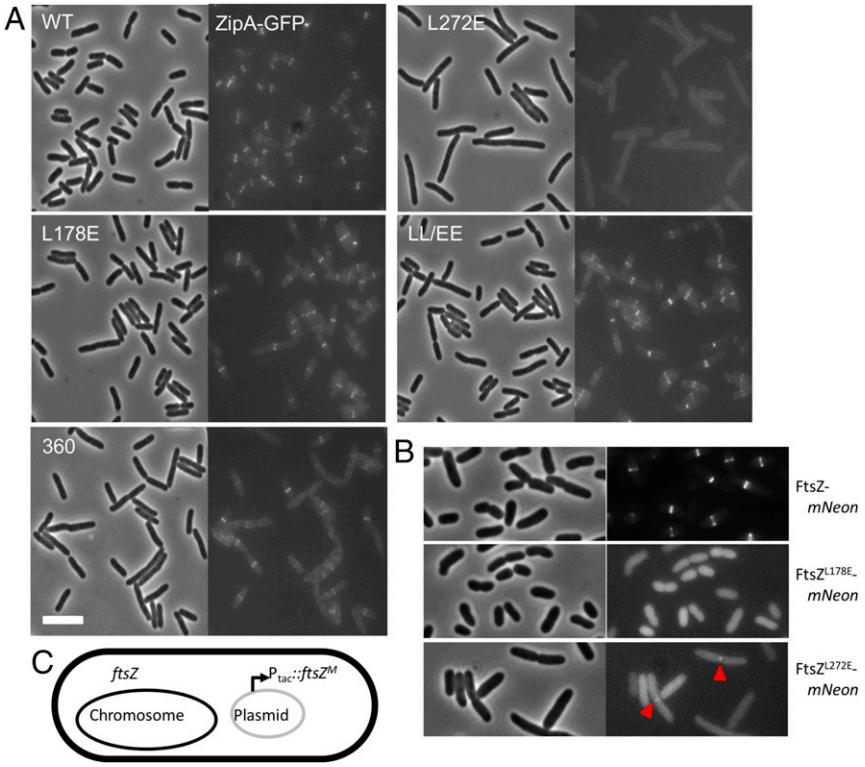

Fig. 3. FtsZ^{L272E} disrupts Z rings and antagonizes FtsZ polymerization. (*A*) FtsZ^{L272E} disrupts Z rings. Exponentially growing cultures of W3110 carrying derivatives of pSEB135 (pBAD18, P_{ara}::*ftsZ*) with various *ftsZ* alleles and pSEB206 (pEXT22, P_{tac}::*zipA-gfp*) growing in LB with 30 μM IPTG were induced for 2 h with 0.05% arabinose, and samples were visualized by fluorescence microscopy to assess ZipA-GFP localization (as a proxy for Z rings). (Scale bar: 5 μm.) (*B*) FtsZ^{L272E} localizes to Z rings. FtsZ^{L272E}-mNeon was observed in constricting cells whereas FtsZ^{L178E}-mNeon did not localize. Samples of transformants of JS238 with derivatives of pSD334 (P_{tac}::*ftsZ*) with various alleles of *ftsZ* were taken from the selection plates (with 0.2% glucose) while the colonies were still small and visualized by fluorescence microscopy. (Scale bar: 3 μm.) (*C*) Diagram of the constructs used. WT *ftsZ* is on the chromosome, and the FtsZ indicated in *A* and *B* was induced from the plasmid.

Effect of GTPase Mutant on Toxicity of FtsZ^{L272E}. All known inhibitors of FtsZ polymerization require the GTPase activity of FtsZ to antagonize FtsZ polymerization, and a reduction in the GTPase activity (due to mutation) is a nonspecific mechanism resulting in resistance (9). We therefore tested whether FtsZ^{L272E} behaved similarly by testing its effect on FtsZ^{D212N}, which has been previously shown to be competent for polymerization but defective in GTPase activity (34). Importantly, FtsZ^{L272E} did not affect FtsZ^{D212N} sedimentation (*SI Appendix*, Fig. S10), indicating that FtsZ^{L272E} also requires the GTPase activity of FtsZ to antagonize polymerization. To further confirm this, we tested whether expression of a GTPase mutant of FtsZ would provide resistance to the toxicity of FtsZ^{L272E} in vivo. For this we used FtsZ^{D212G} (FtsZ2), which has very low GTPase activity and provides resistance to the well-characterized FtsZ inhibitors SulA and MinC/MinD (35, 36). As shown in Fig. 5*B*, the plasmid expressing *ftsZ* enabled cells to grow at 30 μM IPTG, but the presence of *ftsZ2* allowed cells to grow at 1 mM IPTG. Thus, increasing the ratio of FtsZ to FtsZ^{L272E} suppresses FtsZ^{L272E} toxicity, but increasing the stability of FtsZ polymers by copolymerization of a mutant with decreased GTPase activity is dramatically more effective.

Discussion

FtsZ is an ancient filament-forming protein that undergoes cooperative assembly. FtsZ filaments assemble into the Z ring, which is used by most prokaryotic cells for division (2, 37, 38). FtsZ filaments display treadmilling behavior that is used by bacteria to distribute the septal biosynthetic machinery around the septum (16, 20). Here we show that a bottom-face mutant inhibits division in vivo by incorporating into the Z ring, leading to its dissolution, whereas in vitro this mutant antagonizes FtsZ assembly without inhibiting its GTPase activity. In contrast, a top-face mutant is not toxic and has no effect on FtsZ assembly. Furthermore, such a top-face mutation also eliminates the effects of the bottom-face mutant on cell division as well as FtsZ assembly. These observations are consistent with a bottom-face mutant functioning as a capper that blocks filament growth leading to filament disassembly. Thus, we conclude that FtsZ filaments have opposite kinetic polarity of microtubules (bottom-end growth, Figs. 1*A* and 6).

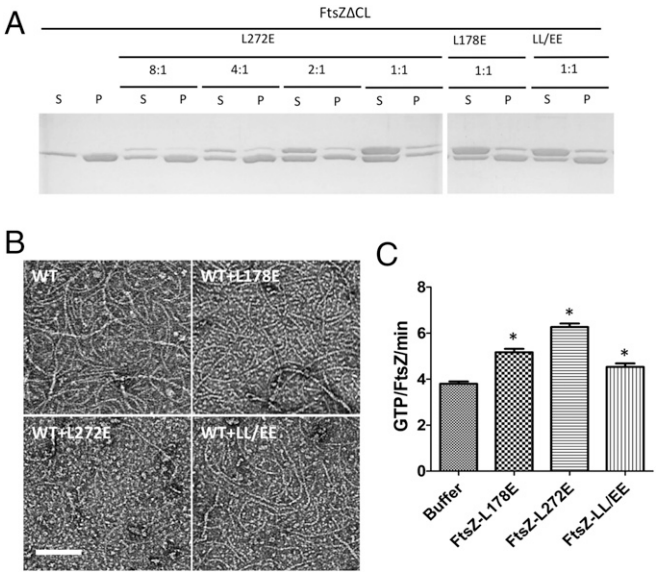

Fig. 4. FtsZ^{L272E} antagonizes FtsZ assembly but enhances its GTPase activity. (*A*) The various FtsZ mutants were added to FtsZΔCL (kept at 5 μM) at the indicated ratios. GTP was added to 1 mM, and after 5 min of incubation the samples were centrifuged and the pellets and supernatants were analyzed by SDS/PAGE. (*B*) FtsZ (2 μM) was mixed with the indicated FtsZ mutants (2 μM) and polymerized by the addition of GTP and examined by negative-stain electron microscopy. (*C*) The various FtsZ mutants were mixed with FtsZ (2 μM) at a 1:1 ratio. GTP was added, and GTPase activity was determined as described in *Materials and Methods*.

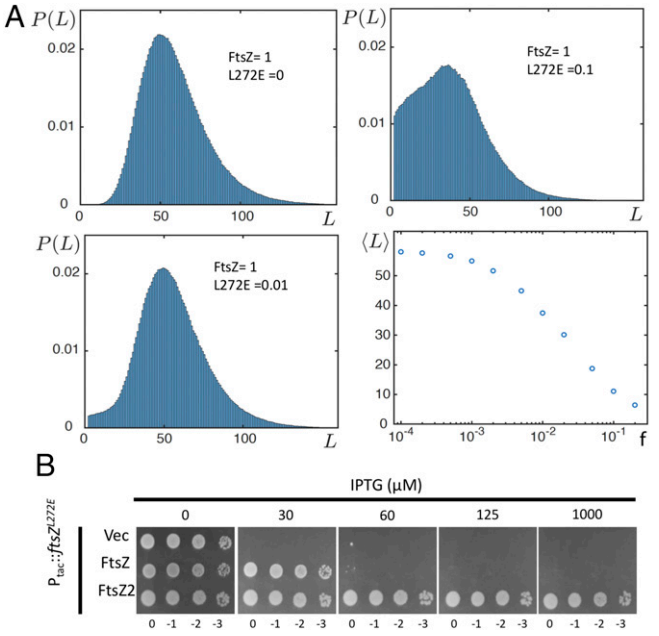

Fig. 5. Modeling the effect of FtsZ^{L272E} on FtsZ polymer length and the effect of increasing FtsZ and decreasing GTPase activity on suppressing FtsZ^{L272E} toxicity. (*A*) Treadmilling model for FtsZ was used to assess the effect of FtsZ^{L272E} on FtsZ filament length with FtsZ polymer-length distribution as a function of the ratio of FtsZ^{L272E} to FtsZ. The fourth panel plots the average polymer length versus the FtsZ^{L272E}-to-FtsZ ratio. (*B*) Increasing FtsZ and reducing GTPase activity suppress the toxicity of FtsZ^{L272E}. JS238/pSD334-L272E (pEXT22, P_{tac}::*ftsZ*^{L272E}) containing plasmids expressing *ftsZ* (pBEF0), *ftsZ*^{D212G} (pBEF2), or a vector control (pGB2) was subjected to a spot test on plates with increasing IPTG.

For a linear filament like FtsZ to undergo cooperative assembly, it was proposed that FtsZ undergoes a conformational switch upon assembly (9, 39, 40). In fact, two conformational forms of FtsZ have been observed: an open form seen when bound to the PC190723 inhibitor and in a filament and a closed form observed in an FtsZ monomer (21, 41). The GTP-bound form of FtsZ exists in these two conformations with the closed conformation the preferred form. Above the critical concentration, sufficient FtsZ exists in the open form to form nuclei consisting of at least a dimer of FtsZ with both subunits in the open form. Based upon our results we propose that the switch to the open form causes the bottom end (T7 end) to have high affinity for the GTP end of another FtsZ molecule, whether it is in the closed or open conformation. This allows an FtsZ monomer in the closed form to add on, which then snaps into the open form, and the process is repeated, resulting in cooperative assembly (Fig. 6). FtsZ^{L272E} can add to the end of a filament and snap to the open form, but subsequent addition is blocked by the substitution, causing it to act as a cap. This cap persists until the filament disassembles, making it possible to detect FtsZ^{L272E} at the Z ring despite its toxicity. In contrast, FtsZ^{L178E} can participate only in nucleation of a filament (the first subunit only), but due to treadmilling is also the first to disassemble, making it difficult to detect at the Z ring.

The above model is also consistent with the effect of the known FtsZ inhibitors MciZ and SulA. MciZ prevents or dismantles Z rings in the mother cell following asymmetric septation during sporulation in *Bacillus subtilis* by reducing the average length of FtsZ filaments by 50% (10, 42). From the crystal structure of the MciZ–FtsZ complex it is clear that MciZ binds to the closed form of FtsZ (10, 42). This suggests that the MciZ–FtsZ complex adds to the end of the filament, which prevents an additional FtsZ subunit from adding on. Thus, an MciZ–FtsZ complex is equivalent to FtsZ^{L272E} (Fig. 6). Previously, it was proposed that MciZ acts primarily by preventing filament annealing (10). Although observed in vitro with purified FtsZ (43, 44), it is not clear whether two membrane-tethered FtsZ filaments would have sufficient mobility to encounter each other in vivo to undergo annealling. SulA, an inhibitor of Z-ring assembly produced in response to DNA damage in *E. coli* (45), has been characterized as sequestering FtsZ since it blocks the GTPase activity (9, 11). However, it is likely that at lower concentrations it functions as a capper as it binds to the same end of FtsZ as MciZ (46). Thus, the FtsZ–SulA complex would also mimic FtsZ^{L272E}.

Both FtsZ^{L272E} and MciZ cause a collapse of the Z ring due to shortening of FtsZ filaments. The addition of FtsZ2 provides dramatic resistance to FtsZ^{L272E}, indicating that mixing in a GTPase-deficient mutant is sufficient to reduce treadmilling and produce longer filaments to rescue the Z ring. This reduced rate of treadmilling leading to an increased average length of filaments is presumably why reduction in the GTPase activity of FtsZ is a nonspecific mechanism to provide resistance to FtsZ inhibitors (47).

Our finding that FtsZ filaments have the opposite kinetic polarity of microtubules is somewhat surprising, considering that FtsZ and tubulin are related (48). Importantly, the conformational change associated with FtsZ assembly (closed to open form) makes it possible for another FtsZ (closed form) to add to the filament. A conformational change is likely also associated with microtubule assembly because the αβ-tubulin heterodimer has been shown to adopt curved and straight conformations (49). Similar to FtsZ, we propose that an unpolymerized GTP-bound

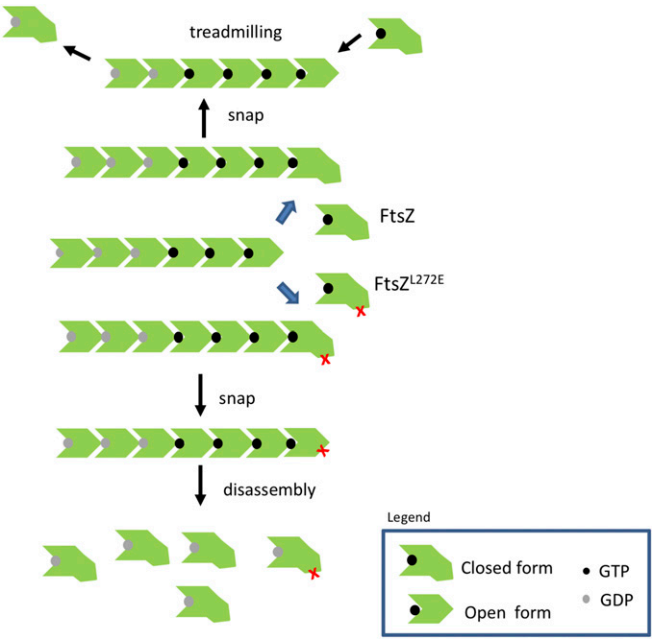

Fig. 6. Model for FtsZ assembly that accounts for the toxicity of FtsZ^{L272E}. FtsZ with GTP bound exists in two conformations, open and closed, with the closed form preferred. Above the critical concentration, two subunits in the open form combine to generate a nucleus, and additional subunits in the closed form add to the bottom end with the energy of binding causing a conformational switch (snap into the open form) to produce a bottom end with high affinity for another GTP-bound subunit. GTP hydrolysis follows assembly resulting in subunits disassociating from the top end, leading to treadmilling. FtsZ^{L272E} adds to the bottom end and snaps into the open form, but subsequent subunit addition is prevented, leading to disassembly of the filament. As subunits disassemble, they return to the closed form and rapidly undergo exchange to the GTP form.

αβ-tubulin heterodimer exists in both the curved and the straight forms with the curved form preferred. A curved αβ-tubulin heterodimer adds to the growing microtubule and snaps into the straight form, which has high affinity for a new incoming curved dimer. This is very similar to FtsZ except that the conformational change in αβ-tubulin is reversed, and assembly results in the generation of a GTP end (β-tubulin) with high affinity for the T7 end of an incoming subunit (α-tubulin). The employment of a polymerization-induced conformational switch to generate kinetic polarity is likely conserved in other members of the FtsZ/tubulin family, such as TubZ, PhuZ, and CetZ, as recently suggested (21). Examining the effect of interface mutants with FtsZ as we have done here should allow determination of the kinetic polarity of such filaments, and this approach can also be employed to determine the kinetic polarity of other filament-forming proteins.

Materials and Methods

SI Appendix, Materials and Methods, contains descriptions of bacterial strains, plasmids, strain and plasmid construction, growth conditions, and procedures. *SI Appendix, Materials and Methods*, also contains procedures for complementation assay, immunofluorescence microscopy, bacterial two-hybrid assays, visualization of GFP fusion proteins, GTPase assay, purification of FtsZ and mutants, sedimentation and electron microscopy assays for FtsZ polymerization, and Western blot. It also contains a section on the simulation of FtsZ treadmilling. The bacterial strains and plasmids used in this study are listed in *SI Appendix*, Table S1, and the oligonucleotide primers are listed in *SI Appendix*, Table S2.

ACKNOWLEDGMENTS. We thank Scott Lovell for the structural overlays and Tom Bernhardt for plasmid pHC892. This work was supported by NIH Grant GM29764 (to J.L.)

1. Wagstaff J, Löwe J (2018) Prokaryotic cytoskeletons: Protein filaments organizing small cells. *Nat Rev Microbiol* 16:187–201.
2. Bi EF, Lutkenhaus J (1991) FtsZ ring structure associated with division in Escherichia coli. *Nature* 354:161–164.
3. Mukherjee A, Lutkenhaus J (1994) Guanine nucleotide-dependent assembly of FtsZ into filaments. *J Bacteriol* 176:2754–2758.
4. Löwe J, Amos LA (1998) Crystal structure of the bacterial cell-division protein FtsZ. *Nature* 391:203–206.
5. Erickson HP, Anderson DE, Osawa M (2010) FtsZ in bacterial cytokinesis: Cytoskeleton and force generator all in one. *Microbiol Mol Biol Rev* 74:504–528.
6. Du S, Lutkenhaus J (2017) Assembly and activation of the Escherichia coli divisome. *Mol Microbiol* 105:177–187.
7. Lutkenhaus J (2007) Assembly dynamics of the bacterial MinCDE system and spatial regulation of the Z ring. *Annu Rev Biochem* 76:539–562.
8. Bi E, Lutkenhaus J (1993) Cell division inhibitors SulA and MinCD prevent formation of the FtsZ ring. *J Bacteriol* 175:1118–1125.
9. Dajkovic A, Mukherjee A, Lutkenhaus J (2008) Investigation of regulation of FtsZ assembly by SulA and development of a model for FtsZ polymerization. *J Bacteriol* 190:2513–2526.
10. Bisson-Filho AW, et al. (2015) FtsZ filament capping by MciZ, a developmental regulator of bacterial division. *Proc Natl Acad Sci USA* 112:E2130–E2138.
11. Chen Y, Milam SL, Erickson HP (2012) SulA inhibits assembly of FtsZ by a simple sequestration mechanism. *Biochemistry* 51:3100–3109.
12. Mukherjee A, Lutkenhaus J (1998) Dynamic assembly of FtsZ regulated by GTP hydrolysis. *EMBO J* 17:462–469.
13. Chen Y, Erickson HP (2005) Rapid in vitro assembly dynamics and subunit turnover of FtsZ demonstrated by fluorescence resonance energy transfer. *J Biol Chem* 280: 22549–22554.
14. Desai A, Mitchison TJ (1997) Microtubule polymerization dynamics. *Annu Rev Cell Dev Biol* 13:83–117.
15. Huecas S, et al. (2008) Energetics and geometry of FtsZ polymers: Nucleated self-assembly of single protofilaments. *Biophys J* 94:1796–1806.
16. Yang X, et al. (2017) GTPase activity-coupled treadmilling of the bacterial tubulin FtsZ organizes septal cell wall synthesis. *Science* 355:744–747.
17. Strauss MP, et al. (2012) 3D-SIM super resolution microscopy reveals a bead-like arrangement for FtsZ and the division machinery: Implications for triggering cytokinesis. *PLoS Biol* 10:e1001389.
18. Mitchison T, Kirschner M (1984) Dynamic instability of microtubule growth. *Nature* 312:237–242.
19. Loose M, Mitchison TJ (2014) The bacterial cell division proteins FtsA and FtsZ self-organize into dynamic cytoskeletal patterns. *Nat Cell Biol* 16:38–46.
20. Bisson-Filho AW, et al. (2017) Treadmilling by FtsZ filaments drives peptidoglycan synthesis and bacterial cell division. *Science* 355:739–743.
21. Wagstaff JM, et al. (2017) A polymerization-associated structural switch in FtsZ that enables treadmilling of model filaments. *MBio* 8:e00254-17.
22. Redick SD, Stricker J, Briscoe G, Erickson HP (2005) Mutants of FtsZ targeting the protofilament interface: Effects on cell division and GTPase activity. *J Bacteriol* 187: 2727–2736.
23. Osawa M, Erickson HP (2005) Probing the domain structure of FtsZ by random truncation and insertion of GFP. *Microbiology* 151:4033–4043.
24. Arumugam S, Petrašek Z, Schwille P (2014) MinCDE exploits the dynamic nature of FtsZ filaments for its spatial regulation. *Proc Natl Acad Sci USA* 111:E1192–E1200.
25. Li Y, et al. (2013) FtsZ protofilaments use a hinge-opening mechanism for constrictive force generation. *Science* 341:392–395.
26. Ortiz C, Natale P, Cueto L, Vicente M (2016) The keepers of the ring: Regulators of FtsZ assembly. *FEMS Microbiol Rev* 40:57–67.
27. Wang X, Huang J, Mukherjee A, Cao C, Lutkenhaus J (1997) Analysis of the interaction of FtsZ with itself, GTP, and FtsA. *J Bacteriol* 179:5551–5559.
28. Guzman LM, Belin D, Carson MJ, Beckwith J (1995) Tight regulation, modulation, and high-level expression by vectors containing the arabinose PBAD promoter. *J Bacteriol* 177:4121–4130.
29. Shaner NC, et al. (2013) A bright monomeric green fluorescent protein derived from Branchiostoma lanceolatum. *Nat Methods* 10:407–409.
30. Du S, Park KT, Lutkenhaus J (2015) Oligomerization of FtsZ converts the FtsZ tail motif (conserved carboxy-terminal peptide) into a multivalent ligand with high avidity for partners ZipA and SlmA. *Mol Microbiol* 95:173–188.
31. Erlenkämper C, Kruse K (2009) Uncorrelated changes of subunit stability can generate length-dependent disassembly of treadmilling filaments. *Phys Biol* 6:046016.
32. Erlenkämper C, Kruse K (2013) Treadmilling and length distributions of active polar filaments. *J Chem Phys* 139:164907.
33. Bi E, Lutkenhaus J (1990) FtsZ regulates frequency of cell division in Escherichia coli. *J Bacteriol* 172:2765–2768.
34. Cho H, McManus HR, Dove SL, Bernhardt TG (2011) Nucleoid occlusion factor SlmA is a DNA-activated FtsZ polymerization antagonist. *Proc Natl Acad Sci USA* 108: 3773–3778.
35. Bi E, Lutkenhaus J (1990) Analysis of ftsZ mutations that confer resistance to the cell division inhibitor SulA (SfiA). *J Bacteriol* 172:5602–5609.
36. Mukherjee A, Saez C, Lutkenhaus J (2001) Assembly of an FtsZ mutant deficient in GTPase activity has implications for FtsZ assembly and the role of the Z ring in cell division. *J Bacteriol* 183:7190–7197.
37. Margolin W (2000) Themes and variations in prokaryotic cell division. *FEMS Microbiol Rev* 24:531–548.
38. Margolin W (2005) FtsZ and the division of prokaryotic cells and organelles. *Nat Rev Mol Cell Biol* 6:862–871.
39. Miraldi ER, Thomas PJ, Romberg L (2008) Allosteric models for cooperative polymerization of linear polymers. *Biophys J* 95:2470–2486.
40. González JM, et al. (2003) Essential cell division protein FtsZ assembles into one monomer-thick ribbons under conditions resembling the crowded intracellular environment. *J Biol Chem* 278:37664–37671.
41. Matsui T, Han X, Yu J, Yao M, Tanaka I (2014) Structural change in FtsZ induced by intermolecular interactions between bound GTP and the T7 loop. *J Biol Chem* 289: 3501–3509.
42. Handler AA, Lim JE, Losick R (2008) Peptide inhibitor of cytokinesis during sporulation in Bacillus subtilis. *Mol Microbiol* 68:588–599.
43. Chen Y, Erickson HP (2009) FtsZ filament dynamics at steady state: Subunit exchange with and without nucleotide hydrolysis. *Biochemistry* 48:6664–6673.
44. Mingorance J, et al. (2005) Visualization of single Escherichia coli FtsZ filament dynamics with atomic force microscopy. *J Biol Chem* 280:20909–20914.
45. Huisman O, D'Ari R (1981) An inducible DNA replication-cell division coupling mechanism in E. coli. *Nature* 290:797–799.
46. Cordell SC, Robinson EJ, Lowe J (2003) Crystal structure of the SOS cell division inhibitor SulA and in complex with FtsZ. *Proc Natl Acad Sci USA* 100:7889–7894.
47. Dai K, Mukherjee A, Xu Y, Lutkenhaus J (1994) Mutations in ftsZ that confer resistance to SulA affect the interaction of FtsZ with GTP. *J Bacteriol* 176:130–136.
48. Nogales E, Downing KH, Amos LA, Löwe J (1998) Tubulin and FtsZ form a distinct family of GTPases. *Nat Struct Biol* 5:451–458.
49. Brouhard GJ, Rice LM (2014) The contribution of αβ-tubulin curvature to microtubule dynamics. *J Cell Biol* 207:323–334.